(3) Errata: Heatley, F.; Bendler, J. T. *Polymer* **1979**, *20*, 1578.
(4) Heatley, F.; Cox, M. *Polymer* **1977**, *18*, 225.
(5) Mashimo, S.; Shinohara, K. *J. Phys. Soc. Jpn.* **1973**, *34*, 1141.
(6) Valeur, B.; Jarry, J. P.; Gêny, F.; Monnerie, L. *J. Polym. Sci., Polym. Phys. Ed.* **1975**, *13*, 667, 675.
(7) Valeur, B.; Jarry, J. P.; Gêny, F.; Monnerie, L. *J. Polym. Sci., Polym. Phys. Ed.* **1975**, *13*, 2251.
(8) Jones, A. A.; Robinson, G. L.; Gerr, F. E. *ACS Symp. Ser.* **1979**, *No. 103*, 271.
(9) Lauprêtre, C. N.; Monnerie, L. *J. Polym. Sci., Polym. Phys. Ed.* **1977**, *15*, 2127, 2143.
(10) Heatley, F.; Begum, A. *Polymer* **1976**, *17*, 399.
(11) Heatley, F.; Cox, M. *Polymer* **1977**, *18*, 399.
(12) Heatley, F.; Begum, A.; Cox, M. *Polymer* **1977**, *18*, 637.
(13) Gêny, F.; Monnerie, L. *J. Polym. Sci., Polym. Phys. Ed.* **1977**, *15*, 1.
(14) Valeur, B.; Monnerie, L. *J. Polym. Sci., Polym. Phys. Ed.* **1976**, *14*, 11, 29.
(15) We used a nonlinear least-squares fit: IMSL program ZXSSQ, "IMSL Library Reference Manual", IMSL L1B7-0005, International Mathematical and Statistical Libraries, Inc., Houston, Texas.
(16) See, however, errata ref 3.
(17) Flory, P. "Statistical Mechanics of Chain Molecules"; Interscience: New York, 1969.
(18) Skolnick, J.; Helfand, E. *J. Chem. Phys.* **1980**, *72*, 5489.
(19) Cole, K. S.; Cole, R. H. *J. Chem. Phys.* **1941**, *9*, 341. *Ibid.* **1942**, *10*, 98.

Some Molecular Motions in Epoxy Polymers: A ^{13}C Solid-State NMR Study

Allen N. Garroway,* William M. Ritchey,† and William B. Moniz

Chemistry Division, Naval Research Laboratory, Washington, D.C. 20375, and Chemistry Department, Case Western Reserve University, Cleveland, Ohio 44106.
Received October 8, 1981

ABSTRACT: ^{13}C NMR solid-state spectra have been obtained over the temperature range 150–350 K for four cured epoxy polymers. Each is the diglycidyl ether of bisphenol A (DGEBA) reacted respectively with (i) piperidine, (ii) *m*-phenylenediamine, (iii) hexahydrophthalic anhydride, and (iv) nadic methyl anhydride. These spectra are compared to the spectra of the unreacted DGEBA monomer, in both crystalline and amorphous forms. The polycrystalline DGEBA ^{13}C spectrum suggests that there is more than one monomer conformation or configuration within the unit cell. This is consistent with X-ray structural assignment, which finds that only one stereoisomer is present but that one end of the monomer is slightly disordered so that either of two possible conformations is possible for the epoxide ring. The origins of some of the observed chemical shift splittings are tentatively assigned. The temperature dependence of the spectra of the piperidine-cured epoxy is analyzed. The rotation by 180° of the phenylene rings accounts for the observed coalescence of certain spectral lines. Analysis of the motion by a single relaxation time model suggests a non-Arrhenius process; this behavior is, however, an artifact of the assumption of a single relaxation time. The full temperature dependence is better described by invoking a distribution of correlation times or, equivalently (vide infra), a nonexponential autocorrelation function. The autocorrelation function $\Phi(t) \propto \exp[-(t/\tau_p)^\alpha]$ ($0 < \alpha \leq 1$ and τ_p given by an Arrhenius relation) is used both for these NMR results and for existing dynamical mechanical results for the piperidine-cured epoxy. Analysis with this correlation function is particularly simple in the $\alpha = 0$ limit, as shown. The NMR line shape is critically sensitive to whether the distribution is *inhomogeneous*, arising from a true (spatially varying) distribution of single-exponential processes, or *homogeneous*, with a nonexponential autocorrelation function which describes all common molecular processes and is independent of position. The NMR results are consistent with the activation energy (E = 63 kJ/mol, 15 kcal/mol) and width parameter ($\alpha = 0.28 \pm 0.02$) found by mechanical spectroscopy, but the 180° flipping of the phenylene ring detected by NMR is either approximately 3000 times slower (inhomogeneous distribution) or 20 times slower (homogeneous distribution) than that for the motion that accounts for mechanical loss. However, the NMR and mechanical relaxation results can be reconciled by presuming that the phenylene rings reorient by small diffusive steps. A reorientation of the phenylene ring by about 3° (inhomogeneous distribution) or 40° (homogeneous distribution) has the same correlation time as the mechanical relaxation process and suggests that small-angle phenylene reorientation occurs with or may be identical with the mechanical relaxation process.

Introduction

The mechanical loss spectrum of a polymer gives a fair overall picture of the frequency and temperature dependence of those molecular motions that couple to an applied stress field. On its own, mechanical spectroscopy does not identify which chemical moieties actually participate in the loss mechanism; such information can sometimes be indirectly inferred from extensive studies[1] of homologous systems. Nuclear magnetic resonance can provide more specific information about the nature of molecular motions. There is, however, no guarantee that motions detected by NMR can actually couple mechanically.

We present here a variable-temperature ^{13}C solid-state NMR study of four epoxy polymers. In the polymers, certain of the resonance lines are found to split below room temperature. In this paper we first examine the origin of these solid-state line splittings. In the solid state, rapid interconversion among many molecular conformations is precluded and resonance lines arise from crystallographically equivalent carbons, rather than chemically equivalent carbons as in the liquid. To refine this point, ^{13}C spectra of four phases of the DGEBA resin are compared: liquid, crystalline, amorphous, and polymerized. A tentative assignment of some of the solid-state splittings in the DGEBA crystal is made by appeal to the crystal structure determined by an X-ray study.[2] A model for steric hindrance that predicts how the ^{13}C chemical shift is perturbed by crowding of the C–H bonds is used to

*To whom correspondence should be addressed at the Naval Research Laboratory.
†Case Western Reserve University

estimate the magnitude of the solid-state shifts.

The best resolved polymer spectra are those of the piperidine-cured system and we examine that system in detail. We find that the observed coalescence of the resonance lines in the polymer points unambiguously to 180° rotation of the phenylene ring; the 180° reorientation may well proceed by small diffusive steps as we later indicate. Such phenylene reorientation probably occurs in the other epoxies studied, but evidence is less direct. The dynamics of the phenylene reorientation are extracted for two models of molecular motion. A simple single relaxation time model with an Arrhenius relation does not fit the data at all temperatures; instead a rather broad distribution of correlation times is required for the full temperature range. We also use the same form of the distribution of relaxation times to describe the existing dynamic mechanical loss spectrum in order to compare the mechanical loss and NMR data.

A distribution of correlation times is formally equivalent to an autocorrelation function that decays nonexponentially. Somewhat arbitrarily, we have selected a model for the motion in which the autocorrelation function $\Phi(t)$ decays as $\exp[-(t/\tau_p)^\alpha]$, where α is a width parameter ($0 < \alpha \leq 1$) and τ_p is a correlation time which we further presume to have a simple Arrhenius behavior, $\tau_p = \tau_0 \cdot \exp(E/RT)$. This functional form was introduced by Williams and Watts[3] to fit the dielectric response of polymers at the glass point. Recently, Ngai and White argued that such a decay function arises naturally from consideration of the spectrum of low-lying excitations in condensed systems and is indeed a very general feature in the solid state.[4] Exhaustive comparison[5] with results from different spectroscopies and diverse physical systems, including polymers, indicates that the response follows this predicted universal relationship. In this paper, however, we take a more limited viewpoint: the functional form $\exp[-(t/\tau_p)^\alpha]$ provides an economical description for our data and a common framework for comparing mechanical relaxation and the present NMR data. It is convenient[6] to represent this autocorrelation function as arising from a distribution of single relaxation time (Debye) processes. We find that the function describing this distribution (indeed, all associated functions) takes on a particularly simple form in the $\alpha = 0$ limit. This limit is in fact a good approximation for α as large as 0.3 or so.

We examine the NMR line shape for chemically exchanging species (which pertains to the case of 180° phenylene ring reorientation) for two classes of relaxation time distributions. The correlation times extracted from the line shape analysis are quite different and depend on whether distribution is inhomogeneous (reflecting a spatial variation of the single relaxation time processes) or homogeneous (indicating a nonexponential autocorrelation function that describes a fundamental molecular process). We then inquire how the 180° flipping of the phenylene ring detected by NMR is related to the β-relaxation process determined by mechanical spectroscopy.

Experimental Section

Materials. Four epoxy polymers were prepared from commercial DGEBA (Dow DER 332). The proportions (in weight percent) and curing schedules were as follows: (i) piperidine (PIP), 5.0%, 393 K for 16 h; (ii) *m*-phenylenediamine (MPDA), 13.7%, 293 K for 15 h, 339 K for 1 h, 422 K for 3 h; (iii) hexahydrophthalic anhydride (HHPA), 31.1%, and *N,N*-dimethylbenzylamine (DMBA), 0.2%, 323 K for 16 h, 363 K for 2 h, 393 K for 2 h; (iv) nadic methyl anhydride (NMA), 46.2%, and *N,N*-dimethylbenzylamine (DMBA), 0.8%, 380 K for 2 h, 408 K for 2 h, 439 K for 2 h. In the text the polymer is referred to by the abbreviated major curing agent, e.g., HHPA.

The crystals of DGEBA (DER 332) had fortuitously grown during a 2-year storage at ambient conditions. Crystals from this batch were used in a related X-ray structural study.[2] The melting point of the crystals was determined as 315.2–315.7 K.

NMR Spectroscopy. All variable-temperature studies were performed on a home-built solid-state ^{13}C spectrometer operated at a field of 1.4 T. For magic angle sample spinning, a modified Lowe[7] geometry with a PTFE through axle was used. To improve the filling factor, the epoxy polymers were cast into molds; the resulting spinners were 12 mm in diameter and 8 mm wide. The crystalline and amorphous resins were run in a hollow Kel-F chamber with a volume of 280 μL. To avoid physical distortion of the epoxies near their glass points by the centrifugal forces, each of the four epoxy specimens was machined into an annulus that just fit into the hollow chamber. These specimens were used for the 350 K spectra. Rotors were spun at a nominal 2 kHz; however, in some cases a substantially slower rate caused large sidebands to appear in the spectra. With this spinner geometry the orientation of the spinning axis reproduces to within about ±1° on changing samples or changing temperature. For amorphous polymers, setting the angle to much better than this accuracy only marginally improves the spectra; for the crystalline specimen much finer control was required. The temperature of the gas for the spinner jet was controlled over the range 150–350 K. Reported "sample" temperatures are actually for the exit gas monitored approximately 2 cm above the axis of the spinner. At low temperatures a nitrogen/helium mixture was used to avoid condensation of the nitrogen in the liquid nitrogen precooler.

All the solid-state spectra presented were obtained by cross polarizing from the spin-locked protons to the spin-locked carbon system under the matched (Hartmann–Hahn[8]) condition. The protons were then decoupled by coherent irradiation. For both cross polarization and decoupling, radio-frequency field amplitudes of about $\gamma B_1/2\pi = 55$ kHz were used; B_1 is the rotating radio-frequency amplitude and γ is the magnetogyric ratio of either spin species. A cross-polarization time of 1 ms was the standard.

A Nicolet NT-150 solid-state spectrometer operating at 3.5 T produced one of the crystalline DGEBA spectra included here (Figure 6). A home-built Beams-Andrew spinner[9] of Delrin was used with a spinning speed of 3.8 kHz.

The liquid-state DGEBA spectrum was run on a JEOL FX60Q spectrometer with acetone as the solvent.

Results

The ^{13}C NMR spectra of the four DGEBA epoxy polymers are shown in Figures 1–4 for the temperature range ca. 150–350 K. Spectra of these epoxies near ambient temperature have appeared earlier.[10,11] The structures in the figures represent DGEBA monomers in which one epoxide group has reacted with the respective curing agent. One of the possible chemical structures formed by polymerization is indicated. Peak assignments are based on liquid-state studies.[12,13] We enumerate the important features of these spectra; later on, they will be discussed in more detail.

For the piperidine-cured epoxy in Figure 1, the methyl peak i broadens at lower temperature and finally disappears, leaving only the unresolved piperidine peaks y and z. The behavior of the methyl peak has been previously discussed for this system:[11,14–16] as methyl reorientation slows and approaches the nutation frequency γB_{1H} of the proton decoupling field, the decoupling process becomes less efficient and the ^{13}C methyl line broadens. The quaternary carbon in the DGEBA backbone is only about 0.21 nm from the methyl protons. As the methyl group slows, the line width of the quaternary carbon resonance h also increases, as shown in Figure 1 at 151 K. Had even lower temperature been accessible, the methyl peak should have reappeared. Such a disappearance and reappearance of the methyl resonance has been observed in poly(methyl methacrylate).[17]

The features central to this paper are seen in Figure 1: the respective coalescences of peaks c and d. At 151 K the

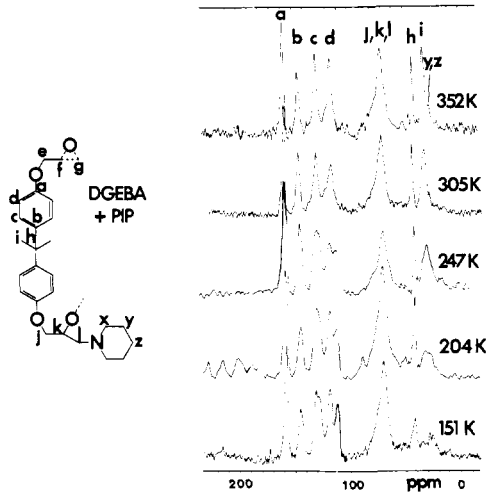

Figure 1. ^{13}C spectra of the epoxy resin diglycidyl ether of bisphenol A (DGEBA) cured with piperidine (PIP) over a 200 K temperature range. In the legend one of the epoxide groups of the monomer is unreacted while the other is shown in one possible structure with the piperidine molecule. (The spinning sidebands in the 204 K spectrum arise from a slower rotation rate and should be ignored.) The coalescences of peak d as well as peak c are analyzed in detail in this paper to provide dynamical information about the nature of phenylene ring reorientation in this epoxy polymer.

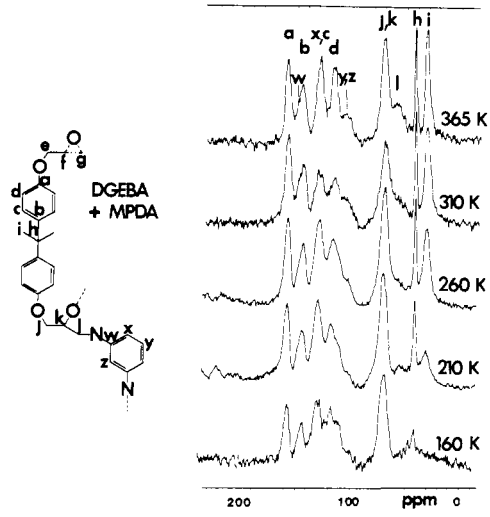

Figure 2. ^{13}C spectra for a DGEBA resin cured with *m*-phenylenediamine (MPDA) over a 200 K range.

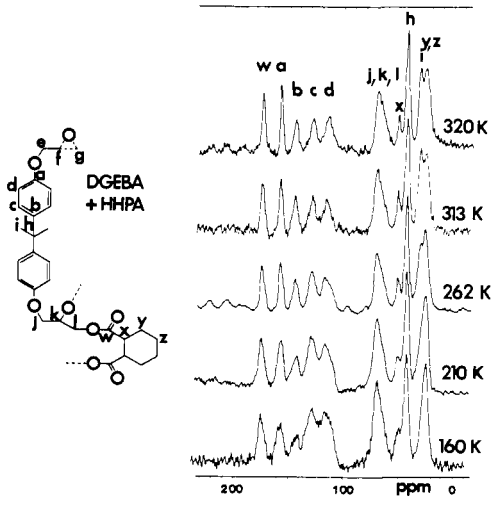

Figure 3. ^{13}C spectra for a DGEBA resin cured with hexahydrophthalic anhydride (HHPA) over a 200 K range.

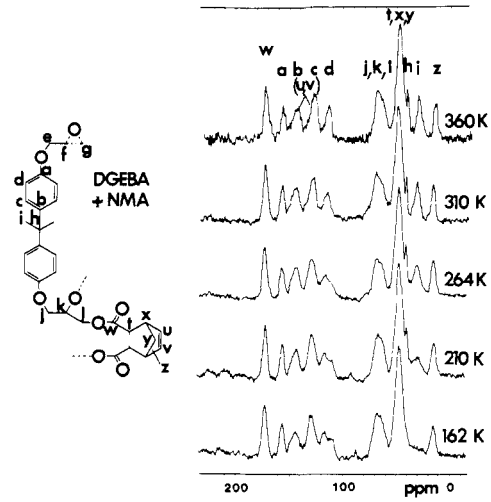

Figure 4. ^{13}C spectra for a DGEBA resin cured with nadic methyl anhydride (NMA) over a 200 K range.

carbons ortho to the oxygen are split into two resolved peaks d with a separation of 7 ppm. The resonance of the meta carbons c is just barely split at 151 K. A spectrum at 175 K, not shown, also indicates the slight splitting in c. (These line shapes are analyzed later on by assuming that at the lowest temperatures each resonance c and d can be represented by a superposition of two Lorentzian lines of equal amplitude but broadened by different transverse relaxation times T_2.) At higher temperatures each set of peaks merges into a single line and that line continues to narrow even at the highest temperature of 352 K.

The coalescence of these resonances suggests the classical chemical exchange process in liquids[18,19] and, for illustration, these spectra will be analyzed later on by means of a simple two-site, single relaxation time exchange model. However, even to the eye, Figure 1 does not present a simple coalescence process: note that a 100 K temperature swing is required to drive the system through partial coalescence, from a broadened, slightly collapsed "doublet" (204 K) to a collapsed line that is still rather broad (305 K). And a much wider temperature is required to complete the coalescence process. For a comparable coalescence point (ca. 273 K) and splitting (7.0 ppm or 105 Hz), the behavior of peak d contrasts to that for a first-order rate process in a liquid, wherein a temperature swing of, say, 50 K would cause a comparable line shape change. Indeed, the doublet d in Figure 1 appears to coalesce by filling in its center, whereas for two-site exchange with a *single* correlation time, the two resonance lines fall toward one another. The filling in at the center of a broader resonance is a characteristic feature of two-site exchange in the presence of a broad distribution of correlation times.[20-22] Accordingly, in the next section the collapse of the doublet is analyzed on the assumption of a distribution of correlation times.

To varying degrees, the low-temperature doublet d also appears in the three other cured epoxies (MPDA, HHPA, and NMA in Figures 2–4). Coalescence of this doublet for the NMA epoxy occurs around 260 K. The coalescence points are not resolved for either the MPDA or HHPA epoxies. As in the piperidine-cured system, in these epoxies the backbone methyl carbon resonance broadens and disappears and the quaternary carbons are also somewhat wider at lowest temperature (ca. 160 K). Note, however, that in Figure 4 the nadic methyl carbon (peak z) broadens only slightly at 162 K while the backbone methyl resonance i has essentially disappeared there. We conclude that the

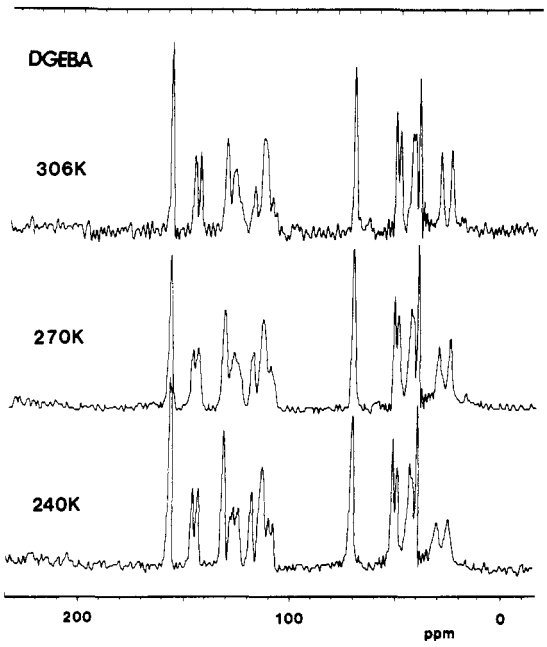

Figure 5. Representative ^{13}C spectra for a polycrystalline powder of DGEBA monomer. See Figure 6 for a DGEBA polycrystalline spectrum at higher magnetic field.

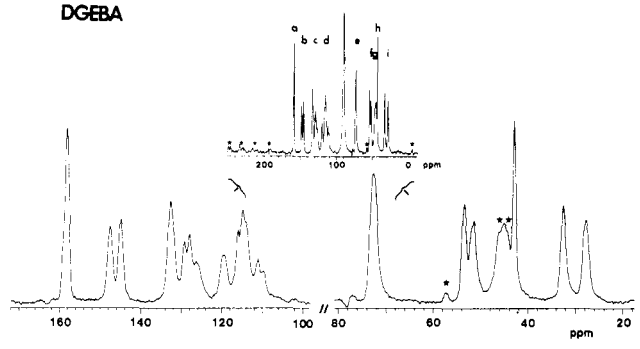

Figure 6. ^{13}C spectrum for polycrystalline DGEBA monomer near 300 K in a 3.5-T field (all other spectra here are for 1.4 T). The insert shows the full spectrum, including a resonance at about 90 ppm from the Delrin rotor. Obvious sidebands are indicated by asterisks.

backbone methyl reorientation is far more hindered than that of the nadic methyl: the backbone methyl group slows down at a higher temperature than the nadic methyl group.

For these epoxies, in common with other glassy polymers, spectral resolution is *generally* best at highest temperature. The issue of resolution in amorphous and crystalline polymers, including, specifically, these epoxies, is elaborated elsewhere.[15,16]

We turn now to the DGEBA monomer. Large single crystals (ca. 2–10-mm linear dimension) grow by sublimation while the monomer is stored at room temperature. A polycrystalline specimen was prepared by compressing a number of these crystals into a hollow rotor. An abbreviated set of temperature-dependent ^{13}C spectra for the crystal monomer is shown in Figure 5. Except for the methyl peaks, there are no significant changes in the spectra in this temperature range. In particular there are no coalescences in the aromatic region as there are in the polymerized phase. For the crystalline specimen the spectral resolution improves at higher magnetic field: the DGEBA spectrum (from the same batch of starting material) is shown in Figure 6 for a static magnetic field of 3.5 T, rather than the 1.4 T for all the other spectra reported here. Sample temperature was not specifically monitored but is estimated to be about 300 K. In Figure 6 the obvious sidebands are indicated by asterisks. The high-field sidebands of the two peaks b probably account for the high- and low-field shoulders on the epoxide peak g.

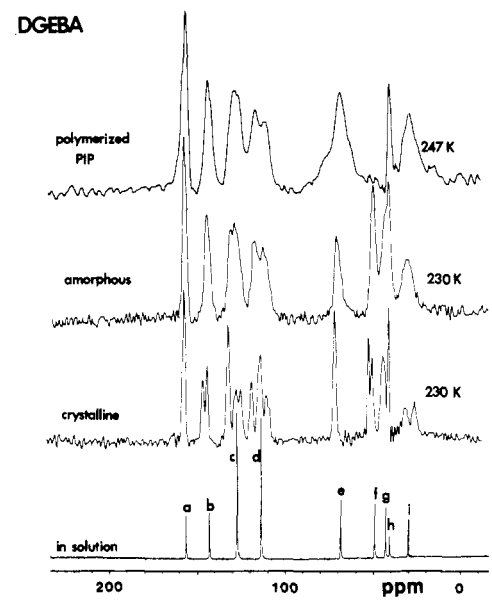

Figure 7. Here ^{13}C spectra of four phases of the DGEBA resin are contrasted. The spectrum for the piperidine-cured polymer is from Figure 1. The solvent peaks have been eliminated in the solution-state spectrum. The lettering of the peaks follows the convention of Figures 1–4.

One striking feature of the crystal-phase spectrum in Figure 6 is the wealth of solid-state splittings. The two methyl resonances are separated by 4.9 ppm. The protonated ring carbons show a number of peaks separated by 6.5 and 10.1 ppm for resonances c and d, respectively. Solid-state splittings of comparable magnitude have been reported earlier in poly(2,6-dimethyl-1,4-phenylene oxide),[23] 1,4-dimethoxybenzene,[24,25] and 1,3,5-trimethoxybenzene.[26] The origin of some of these solid-state splittings in the polycrystalline epoxy monomer will be addressed later on.

Figure 7 compares spectra of different phases of DGEBA. The four phases are polymerized (with piperidine, at 247 K from Figure 1), amorphous (230 K), crystalline (230 K), and liquid (in acetone, solvent peaks deleted). The identical sample was used for both the crystalline and amorphous spectra. After the crystalline spectrum was recorded, the sample rotor, still spinning, was warmed above the DGEBA melting point (315.2–315.7 K) and then cooled. Spinner alignment was later checked and no substantial improvement of the resolution of the amorphous spectrum could be achieved. Apparently, the discrete solid-state splittings, of the order of 5–10 ppm as shown above, are blurred out in the amorphous phase (Figure 7), leading to distributions of isotropic chemical shifts that determine in large measure the achievable resolution in amorphous organic solids.[15,16] In the aromatic region of the spectra, the polymerized and amorphous forms are virtually identical. The major changes in the aliphatic region reflect the chemistry changes during polymerization: resonances from epoxide carbons f and g are shifted downfield and overlap with the methylene resonance. The degree of polymerization can be crudely estimated based on the disappearance of peaks f and g. We infer that less than 5–10% of the epoxide groups are unreacted in this piperidine-cured polymer. An improved signal-to-noise ratio in these spectra would probably reduce this upper bound.

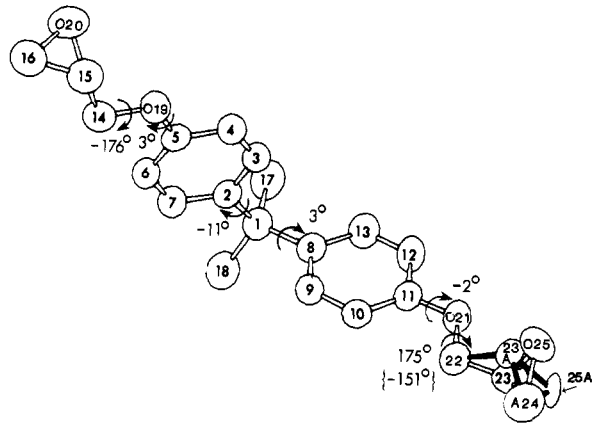

Figure 8. X-ray-determined structure of DGEBA (figure adapted from ref 2). Also shown are selected torsional angles; these indicate the near coplanarity of the methyl, phenylene, and methylene groups. One end of the monomer is apparently disordered; two conformations of one epoxide group are found. In the nonskewed conformation, site A24 is occupied by a carbon atom while in the skewed conformation, shown with bonds darkened, an oxygen is in site A24.

Discussion

We first examine the ^{13}C spectrum of DGEBA in the crystal state. Identification of the solid-state splittings observed in the ^{13}C spectra in the context of the known DGEBA crystal structure will then assist to determine the character of the molecular motions that average out those splittings in the polymer. So that this motion may be directly compared to that responsible for the β peak in the mechanical loss spectra, a parallel analysis of the available mechanical loss data is presented.

DGEBA Crystal Structure. The DGEBA monomer crystallizes by sublimation into monoclinic crystals of space group $P2_1/c$. Cell dimensions[2] are as follows: a = 0.8260 (4) nm, b = 1.1659 (4) nm, c = 2.0228 (6) nm, β = 105.6 (1)°, Z = 4, and d_c = 1.205 (1) g cm^{-3}. The structure is shown in Figure 8. The numbering follows ref 2 and indicates the order in which the heavy-atom positions were identified by the computer algorithm. Torsional angles, indicating deviations from coplanarity, are also shown.

The molecule has twofold symmetry out to the methylene groups C14 and C22. Note that the aromatic rings are canted so that each ring is virtually coplanar with one or the other methyl carbon. The methylene groups are also nearly in the plane of the aromatic ring. However, C22 is trans to the coplanar methyl C17 while methylene C14 is cis to methyl C18. Furthermore, the structure of the epoxide group attached to C22 is apparently disordered. Two conformations were required to allow suitable refinement of the structure.[2] Both share a common atomic position, labeled A24. When this site is occupied by a carbon atom (C24), the epoxide group C23, C24, O25 looks very much like the one at the other end of the monomer: that is, the C22–C23 bond is essentially coplanar with the aromatic ring, and the methylene protons of C22 equally straddle the ring. However, in the alternative structure, darkened in Figure 8, the A24 site is occupied by an oxygen atom (O24) and the epoxide group C23A, C25A, O24 is skewed so that the C22–C23A bond is not in the plane of the aromatic ring. In the X-ray analysis equal numbers of skewed and unskewed epoxide groups were assumed at the disordered end of the molecule. The X-ray study finds that all the asymmetric carbons C15, C23, and C23A have *S* chirality: the skewed and unskewed alternatives for the epoxide structure represent a change in conformation and not configuration. However, the study does note that some *R,S*-type molecules may be undetected because of the disorder in the one epoxide group.

In general, the source of the splittings in solid-state ^{13}C spectra, e.g., Figures 5–7, is not yet established and the full assignment of all the resonances cannot be completed. To see if the *magnitude* of these splittings can be easily estimated, we employ the model of Grant and Cheney[27] to predict how the chemical shift is affected by the crowding of the CH bonds in the solid state. Though the predictions are only modestly in agreement with observation, this model assists in assigning some of the lines in the DGEBA crystal spectrum. Moreover, the model helps to suggest how molecular motion, in particular reorientation of the aromatic ring, will coalesce certain lines by averaging these splittings to zero.

In the steric hindrance model, a CH bond is compressed or expanded by the mutual repulsion of the bonded hydrogen and a nearby nonbonded hydrogen. The shift depends on the hydrogen–hydrogen distance r and the angle θ between the CH bond and the interhydrogen separation vector. Grant and Cheney propose[27]

$$\Delta_c = -1680 \cos\theta \exp(-26.71r) \quad (1)$$

The original expression has been adapted so that r is in nm and Δ_c is the chemical shift difference on the δ_c scale. The net shift for each of the carbons in the DGEBA monomer was calculated by summing the contributions of eq 1 for hydrogen–hydrogen separations out to 0.25 nm; the separations were calculated[28] from the X-ray study of ref 2. Only hindrances particular to the crystalline state were considered; those effects from parts of the molecule that are rigid in the liquid state were ignored. Just the methyl conformation was considered in which each methyl group is oriented so that one methyl hydrogen is trans and two are gauche with respect to the other methyl carbon. The net shifts are displayed in Table I. There the primes refer to carbons that are influenced by the skewed (rather than the unskewed) epoxide group. As there are presumably equal numbers of skewed and unskewed groups, the intensities of the partners in the primed and unprimed pair (e.g., C13′) are each $^1/_2$ while the intensity of a carbon that does not see the disordered epoxide group (e.g., C9) is 1.

The significant feature in the crystalline-state DGEBA spectra of Figures 5–7 is the number of resolved lines for the protonated carbons. In the monomer there are only four carbons meta and four ortho to the oxygen carbon in the two phenylene rings. However, the spectrum of Figure 6 shows four and five (possibly six) lines, respectively. This is direct evidence that more than one conformation or configuration of the monomer is present. Table I also includes the experimental values for the chemical shift difference between the solid-state spectrum of Figure 6 and the corresponding lines in the liquid-state spectrum of Figure 7. Since no attempt was made to account for solvent effects or solid-state effects beyond this very restricted estimate of steric effects, little should be made of the absolute numbers for the chemical shifts.

For the meta carbons (peak c) five lines are predicted in Table I, though there may be some overlap. The methyl protons are primarily responsible for the dominant shifts. C3 is unshifted and the C18 methyl group shifts C7 by −1.7 ppm and C9 by −1.2 ppm. C13 is displaced by −1.5 ppm, but C13′ sees the hydrogen of C25A on the skewed epoxide group and is shifted by −4.5 ppm. We suggest that C13′ accounts for the upfield shoulder at 126.2 ppm in Figure 6.

The ortho carbons (peak d) are split primarily by the methylene groups, as follows. C12 is unshifted. C4 is shifted −2.2 ppm by an intermolecular coupling to a hy-

Table I
Observed and Predicted Solid-State ^{13}C Chemical Shifts in Crystalline DGEBA

	peak								
	a	b	c	d	e	f	g	h	i
observed peak shift,[a] ppm	2.2	4.1 1.7 0.5 −1.4	5.1 1.7 1.0 0.4[c] −2.8 −4.1	6.0 2.1	4.1	3.3 1.4	0.7[d]	1.4	1.6 −3.3
predicted peak shift,[b] ppm	—	—	0 (C3) −1.7 (C7) −1.2 (C9) −1.5 (C13) −4.5 (C13′)	0 (C12) −1.9 (C10) −1.9 (C6) −6.6 (C6′) −2.2 (C4) 0 (C4′)	−2.5[e] (C14) 2.3 (C14′) 2.5 (C22) 2.5 (C22′)	0 (C15) 0 (C23) −3.0 (C23A)	0 (C24) −3.2 (C16) −8.7 (C25A)	—	−1.4 (C18) −2.9 (C17)

[a] Relative to liquid-state DGEBA spectrum (acetone solvent); at ca. 300 K. External references used for both liquid- and solid-state spectra. [b] Steric hindrance model (ref 27). Numbering of carbons follows Figure 8. The prime indicates a carbon influenced by the epoxide group in the skewed conformation. [c] Shoulder of central peak. [d] Peak is rather broad, about 3 ppm wide. [e] Ignores contribution of an intermolecular oxygen 0.214 nm from the methylene hydrogen.

drogen on the unskewed epoxide group; C4′ is unaffected. C10 is shifted −1.9 ppm by the methylene hydrogens on C22, and C6 is also shifted −1.9 ppm by the methylene hydrogens on C14. C6′ sees a skewed epoxide group and is shifted to −6.6 ppm. C6′ may account for the upfield shoulder at 109.7 ppm in Figure 6.

The aliphatic resonances present more of a problem. The methylene carbons are influenced by nearby epoxide groups and the local environment of each methylene group is rather different. Yet the predicted net shift of carbons C14′, C22, and C22′ is about 2.5 ppm. Now C14 is predicted to resonate at −2.5 ppm but is also shifted by an intermolecular epoxide oxygen only 0.232 nm from the methylene hydrogen. In this geometry the electronegative oxygen should produce a positive shift, but its magnitude is unknown. A +5-ppm shift from the crowding by this oxygen would fortuitously cause all the methylene peaks to overlap. Agreement for the epoxide peaks is also ambiguous. Two resonances split by 3 ppm are predicted for peak f but with an intensity of 3/2:1/2 rather than the 1:1 observed. Peak g is rather broad and may have some underlying structure, though as mentioned earlier, the spinning sidebands contribute to the shoulders in peak f in Figure 6. The steric hindrance analysis predicts that C25A should be shifted by −8.7 ppm, but no evidence is found for this large shift. Two peaks separated by 1.5 ppm are predicted for the methyl resonance i; the observed splitting is 4.9 ppm. Nothing is said in the Grant–Cheney model about the shifts for the unprotonated carbons.

This steric hindrance model predicts shifts that are the right order of magnitude as those observed; agreement in detail is not good. The analysis identifies the major shifts to be expected from the skewed epoxide group. The additional peak structure and resolved peaks in the protonated aromatic carbons are broadly consistent with the presence of this disordered epoxide group. However, in the aliphatic region the large shift of −8.7 ppm is not observed for C25A on the skewed epoxide group.

Even without recourse to a model for solid-state splitting, the (high magnetic field) ^{13}C spectrum of Figure 6 shows that more than one conformation or configuration of the monomer is present. One hopes that as experience builds with these solid-state splittings, more crystallographic information can be inferred directly from ^{13}C NMR spectra.

Dynamical Properties. We return now to the collapse of the two low-temperature doublets c and d of the protonated phenylene carbons in the piperidine-cured epoxy and infer the nature of the molecular motions responsible. The analysis is restricted to the piperidine-cured system, since, unfortunately, details of the corresponding coalescenses are obscured for the MPDA, HHPA, and NMA epoxy polymers.

The foregoing arguments based on deshielding by steric hindrance show that both *intra-* and *inter*molecular crowding effects are important: the variation in crowding makes the carbons inequivalent in the solid. (We use the term inequivalent to indicate a difference in chemical shift; strictly speaking, inequivalence refers to variations in the spin–spin coupling while isochronous connotes identical chemical shift.[29]) One motion that accounts for the coalescence observed in Figure 1 is a 180° flipping of the aromatic ring. Return for a moment to the crystal structure diagram in Figure 8. A 180° rotation of a phenylene group is equivalent to a simultaneous interchange of carbons C4–C6 and C3–C7 and similarly for the other ring. This motion simultaneously averages out any intra- or intermolecular splittings, making, say, C4 and C6 equivalent if the rotation is fast enough. We will not attempt at this moment to distinguish between true 180° flips and large angle rotation by diffusive steps but return to this question later. (Adoption of a diffusive-step model would require some knowledge about how the isotropic chemical shift varies away from the 0,180° conformation of the phenylene group.)

We suspect that the splittings in peaks c and d in the amorphous and polymerized phases of the resin arise primarily from intramolecular effects: the intermolecular contributions are probably too diffuse to create such a discrete splitting, as shown in Figure 7. In the polymer and amorphous resin the splitting in d probably arises from the methylene hydrogens while the rather weaker splitting in c is ascribed to the proximity of the methyl hydrogens. If this were the case, then motion of the methylene group about the ether linkage would cause a coalescence of d. However, such motion would leave peak c essentially unaffected, as its splitting derives from the methyl hydrogens. However, it will be shown on the basis of a very simplistic model of exchange that the correlation times for the motion describing the collapse of c and d are identical to within a factor of 2 and therefore it is most likely a common motion that drives the ring carbons.

i. NMR Line Shape Analysis (Single Relaxation Time). A full analysis of the line shape variations with temperature in a solid-state ^{13}C spectrum is a formidable task. Any motion may modulate not only the isotropic

Table II
Two-Site Exchange Parameters[a]

	$\delta\omega/2\pi$, Hz/ppm	T_{2A}, ms	T_{2B}, ms
peak c	65/4.3	5.5	4.8
peak d	105/7.0	5.0	4.0

[a] For the piperidine-cured DGEBA epoxy. Derived by computer simulation to the 151 K spectrum of Figure 1.

chemical shift but also the anisotropic chemical shift and dipolar couplings. These will be reintroduced into the spectrum whenever[15,16] the molecular modulation frequencies become comparable to the magic angle sample spinning frequency or to the decoupling frequency $\gamma_H B_{1H}$. In an amorphous material there is some complex distribution of isotropic chemical shifts that is averaged to greater or lesser extent by the motion and hence can become temperature dependent. The motion may be quite complex, involving many different moieties as well as a distribution of correlation times.

The important features of the motion can be extracted by recourse to a very simplistic model for chemical exchange, appropriate for two-site exchange in liquids. We make the following simplifying assumptions: (i) dipolar and chemical shift anisotropy broadenings are unimportant; (ii) a Lorentzian description of the line shape is appropriate; (iii) the phenylene ring reorients by 180° about the 1,4 axis so that the ring carbons effectively exchange; (iv) the asymmetries in peak heights in the low-temperature doublets (Figure 1) are due to broadening by isotropic chemical shifts and do not indicate different populations.

For exchange between two sites A and B with equal populations but with unequal relaxation times T_{2A} and T_{2B}, the line shape $M(\omega)$ is, adapted from ref 30,

$$M(\omega) = \frac{-2\omega Y + (\zeta^{-1} + \tau_c^{-1})X}{X^2 + Y^2} \qquad (2)$$

where

$$X \equiv (\delta\omega/2)^2 - \omega^2 + (2\tau_c\zeta)^{-1} + (T_{2A}T_{2B})^{-1}$$

$$Y \equiv (\delta\omega/2)(T_{2B}^{-1} - T_{2A}^{-1}) - \omega(\zeta^{-1} + \tau_c^{-1})$$

and

$$\zeta^{-1} \equiv T_{2A}^{-1} + T_{2B}^{-1}$$

Here, $\delta\omega$ is the isotropic chemical shift difference, and resonance offset ω is measured from the center of the two lines A and B. The lifetime of each site is τ_c and is equal to the correlation time for 180° flips of the phenylene group in this application.

We first consider motion described by a single correlation time. This restriction will be relaxed subsequently. The 151 K spectrum of Figure 1 was used to establish values for $\delta\omega$ and T_{2A} and T_{2B}; those are tabulated in Table II. These values are assumed temperature independent and, reassuringly, we find that the 352 K line shape is reasonably well fit by the fast-exchange time limit of a Lorentzian with a relaxation time of 2ζ.

The correlation time for both peaks c and d was independently varied to provide a best fit between the computer-simulated spectrum from eq 2 and each observed spectrum for temperatures between 151 and 352 K. The spectra of Figure 1 were fit, as well as nine other spectra that interleave the temperatures of Figure 1. The experimentally determined correlation times are shown in Figure 9. The representative error bars denote the range for which a reasonable fit to the individual spectrum could

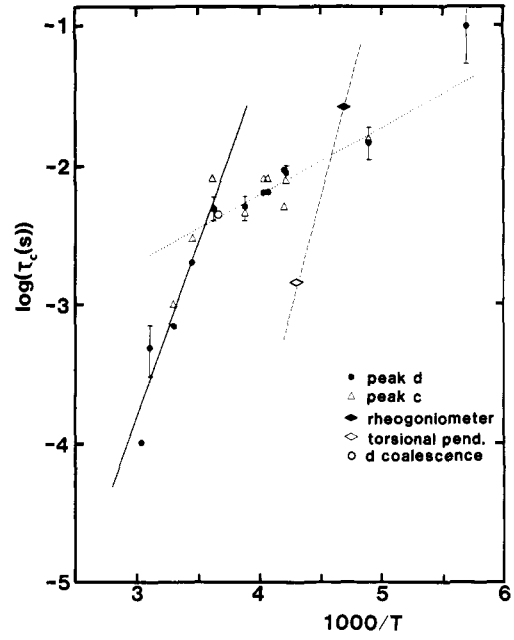

Figure 9. Single-correlation time analysis for the β peak of mechanical relaxation data and the coalescence of peaks c and d of the protonated phenylene carbons in the ^{13}C NMR spectra (Figure 1) for the piperidine-cured DGEBA epoxy. The dashed line represents the temperature dependence (E = 63 kJ/mol; 15 kcal/mol) inferred from rheogoniometer measurements. For the NMR data the temperature dependences of 50 kJ/mol (solid line) and 9 kJ/mol (dotted line) are drawn only as guides for the eye.

be achieved. Since the doublet of peak c is poorly resolved, the scatter in the correlation time for peak c is greater than for peak d; further, at high and low temperatures the correlation time for peak c could not be determined. Even so, at all temperatures the correlation times inferred for the two peaks are the same, to within a factor of 2. This strongly suggests that the ring carbons are suffering a common motion, impressed by a 180° reorientation. At high temperatures, above about 278 K, the correlation time for both peaks c and d follows an Arrhenius relation $\tau_c = \tau_0 \exp(E/RT)$, with E = 50 kJ/mol (12 kcal/mol) and $\tau_0 = 0.8 \times 10^{-12}$ s.

Also shown in Figure 9 are correlation times inferred from mechanical spectroscopies. For this epoxy the β peak has been determined by a rheogoniometer[31,32] and a torsional pendulum.[33] At the peak of the β relaxation, the quoted correlation time is just $\tau_c = (2\pi f)^{-1}$, where the frequencies f are 6 and 110 Hz with β transition temperatures 213 and 240 K, respectively. This expression is appropriate for a single correlation time model; for a distribution of correlation times that is symmetrical in log τ_c, the loss maximum occurs at a frequency corresponding to the mean of the distribution. An asymmetric distribution will be treated later and requires a slightly different expression. Shown too is the temperature dependence as measured in the rheogoniometer experiment; it corresponds to an activation energy of 63 kJ/mol (15 kcal/mol). The determination of this activation energy is discussed later. For the single correlation time model, the Arrhenius prefactor is $\tau_0 = 1 \times 10^{-17}$ s for the rheogoniometer data. In the high-temperature region of Figure 9, the temperature dependencies of the correlation times from the mechanical results (63 kJ/mol) and the ^{13}C spectra (50 kJ/mol) are broadly consistent. At the coalescence point of peak d of 273 K, the correlation time for 180° phenylene jumps is 4.5 ms, 400 times slower than the extrapolated correlation time of 11 μs from the mechanical relaxation data. This disparity is exacerbated by the difference in

activation energies if the Arrhenius prefactors are compared: the prefactors differ by 5 orders of magnitude. The differences will be reconciled later on.

Figure 9 seems to suggest that at lower temperature, below about 278 K, there is a second motion, indicated by the dotted line. However, the apparent activation energy of 9 kJ/mol (2 kcal/mol) and reorientation time prefactor of 65 μs appear quite unphysical. Further, it is too great a coincidence that the crossover temperature separating the fast and slow motions occurs very near to the coalescence temperature, which for peak d corresponds to 273 K with a correlation time of 4.5 ms. (Indeed, Figure 9 helps to quantify the remark made earlier that the coalescence occurs over such a broad temperature range. If only the putative high-temperature mechanism were active, the spectra would undergo these changes over the range 250–350 K rather than 150–350 K.)

However, the behavior below the coalescence point in Figure 9 is an artifact of the single correlation time model. Introduction of a distribution of correlation times gives a more satisfactory fit to these data. It does not, however, remove completely the discrepancy in the magnitude of the correlation time between the mechanical data and the analysis of the NMR data for 180° phenylene group reorientation.

ii. Distribution of Relaxation Times. Various forms for a distribution of relaxation times have been proposed.[34] Such a distribution is *formally* equivalent to a nonexponential decay of the autocorrelation function $\Phi(t)$ describing the motion: starting from either the probability distribution functions $\rho(\tau)$ and $G(\log \tau)$ or the autocorrelation function $\Phi(t)$, the other functions can be defined by

$$\Phi(t) = \int_0^\infty d\tau\, \rho(\tau) \exp[-(t/\tau)] = \int_{-\infty}^{\infty} d(\log \tau)\, G(\log \tau) \exp[-(t/\tau)] \quad (3)$$

Here, $G(\log \tau)$ is just the probability distribution on the logarithmic time axis.

The autocorrelation function considered here is

$$\Phi(t) = N^{-1} \exp[-(t/\tau_p)^\alpha] \quad (4)$$

where $0 < \alpha \leq 1$ and the normalization constant $N = (\tau_p/\alpha)\Gamma(\alpha^{-1})$. Here, Γ denotes the gamma function. This form for $\Phi(t)$ was applied in a study of the dielectric loss at the α peak in poly(ethyl acrylate) by Williams and Watts.[3] Recently, Ngai and White[4] proposed a theory of collective excitations in solids that leads to the same functional form; Ngai[5] reanalyzed an extremely broad body of experimental data and found the data consistent with this autocorrelation function. There are certain virtues of this form of the correlation function. The shape of the distribution is determined just by α. The position of the distribution on the time axis is determined by τ_p. On the logarithmic time axis the distribution is asymmetric for $\alpha < 1$. (The $\alpha = 1$ limit simply recovers the single relaxation time behavior.) One consequence of the asymmetric distribution is that the imaginary part of the dielectric response ϵ'' varies as $\omega^{-\alpha}$ at high frequency and as ω^{+1} at sufficiently low frequency, in keeping with experimental results.[5] The temperature dependence must be inserted into τ_p and we take a simple Arrhenius form

$$\tau_p = \tau_0 \exp(E/RT) \quad (5)$$

(In the discussion of Ngai and White,[4,5] both the temperature dependence and τ_0 are introduced and interpreted somewhat differently than here.) The width of the distribution of relaxation times is temperature independent: a change in temperature produces only a uniform logarithmic shift of the relaxation times. In contrast, however, the width of the distribution is temperature dependent in, say, a model in which a normal distribution of activation energies leads by the Arrhenius relation to a log-normal distribution of relaxation times.[20,21,35]

For the Williams–Watts form of the autocorrelation function, both the probability distribution density $\rho(\tau)$ and the imaginary part $G''(\omega)$ of the mechanical compliance will be useful here. An explicit form for the density is[6]

$$\rho(\tau) = \frac{1}{\pi\tau} \sum_0^\infty (-1)^{k+1} \frac{\Gamma(1 + k\alpha)}{k!} \left(\frac{\tau}{\tau_p}\right)^{k\alpha} \sin(\pi k\alpha) \quad (6)$$

For the imaginary part of the mechanical response, we adapt the expression for the dielectric loss[6,36] to the mechanical loss case:

$$\frac{G''(\omega)}{G_U - G_R} = \sum_1^\infty (-1)^{k+1} \frac{\Gamma(1 + k\alpha)}{k!} \left(\frac{1}{\omega\tau_p}\right)^{k\alpha} \sin(\pi k\alpha/2) \quad (7)$$

where G_R and G_U are the relaxed and unrelaxed moduli, respectively. (Reference 36 also provides an expansion for the dielectric loss that converges rapidly for low frequency, while the above expressions converge more readily at higher frequency.)

Equation 7 is rather unwieldy. We find eq 7 has a simple form in the limit of very broad distribution ($\alpha = 0$):

$$\lim_{\alpha \to 0} \frac{G''(\omega)}{G_U - G_R} = \left(\frac{\pi}{2}\right) \alpha (\omega\tau_p)^{-\alpha} \exp[-(\omega\tau_p)^{-\alpha}] \quad (8)$$

In this limit the maximum in $G''(\omega)$ occurs for $\alpha \ln \omega\tau_p = 0$. The frequencies $\omega_\pm$ at the half-maximum points of eq 8 are found from

$$\pm\alpha \ln \omega_\pm\tau_p + \exp[\mp(\alpha \ln \omega_\pm\tau_p)] = 1 + \ln 2 \quad (9)$$

From eq 9 the full width of $G''(\omega)$ at half-height in decades of frequency is approximately $1.062/\alpha$.

We can now develop a rule of thumb for determining α from the width of $G''(\omega)$, valid for all values of α. In general, in the limit of a broad distribution of relaxation times, the out-of-phase component $G''(\omega)$ of the susceptibility takes on the same shape as the relaxation time distribution[37] provided ω is substituted for τ^{-1}. This can be shown explicitly for this distribution from eq 6. Hence in this same limit the width of the relaxation time distribution is also $1.062/\alpha$, in decades of relaxation time. On the other hand, in the $\alpha = 1$ (single relaxation time) limit, the width of the response curve is 1.14 decades. Our explicit computer calculation of eq 7 shows that the actual width of $G''(\omega)$ varies monotonically from the $\alpha = 1$ (1.14 decades wide) to $\alpha = 0$ ($1.062/\alpha$ decades wide) limits. If we employ the relation that $\alpha \simeq 1.1/W$, where W is the full width at half-height (in decades) for the imaginary part of the susceptibility, then from only the width of the response curve $G''(\omega)$ we can estimate α to within about 5% for all values of α between 0 and 1.

We first analyze available mechanical loss data and then the ^{13}C NMR line shape for two-site exchange driven by a distribution of correlation times.

iii. Mechanical Relaxation Analysis. Figure 10 shows rheogoniometer data for the frequency dependence of G'', the imaginary component of the modulus for a piperidine-cured DGEBA resin. This figure is adapted from Figure 8 of ref 31. The starting materials and curing schedule for the mechanical specimen were the same as for the NMR specimens. This master curve reproduced

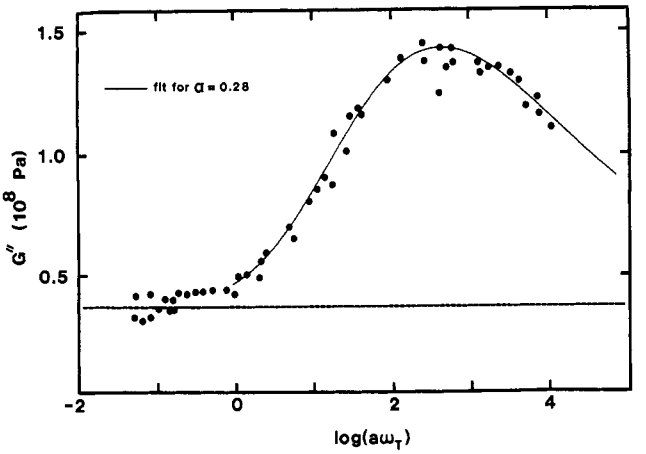

Figure 10. Master curve for the β-relaxation peak determined by rheogoniometer measurements of DGEBA cured with piperidine (adapted from ref 31). The imaginary part of the storage modulus is plotted against the shift factor a at 223 K. Shown is a theoretical fit with a Williams–Watts form of the time autocorrelation function (width parameter $\alpha = 0.28$). A frequency-independent base line (dashed line) is assumed to facilitate the fit.

in Figure 10 was constructed from loss data taken over $3^1/_2$ decades of frequency. Temperature was changed and the shift factor determined to bring the frequency data onto the master curve.[31,32] The shift factor fits an Arrhenius relation over the temperature range studied (200–256 K), with an activation energy of 63 kJ/mol (15 kcal/mol). The continuous curve in Figure 10 is the computer-generated fit for eq 7 using the Williams–Watts form of the autocorrelation function. (The solid curve in the original figure[31] is a guide for the eye and is not this calculated curve.) Best fit is achieved for $\alpha = 0.28 \pm 0.02$. Since the experimental values for the modulus G'' do not go to zero at low frequency, a base line contribution was assumed and is indicated by the dashed curve in Figure 10. At 6 Hz the maximum in tan δ occurs at about 213 K, and with the supplied values[31,32] of G', we estimate the maximum in G'' occurs at about 208 K. The maximum in the imaginary part of the susceptibility is at $\omega\tau_p = k(\alpha)$, where $k(\alpha)$ is a factor less than 1 and depends weakly[38] on α. For $\alpha = 0.3$, $\omega\tau_p = 0.639$ and the mechanical data give the value $\tau_p = 17$ ms at 208 K.

iv. NMR Line Shape Analysis (Distribution of Relaxation Times). We now conduct a parallel analysis of the ^{13}C two-site exchange line shape for the phenylene carbon ortho to the oxygen, peak d in the figures. At this point, we must make an essential distinction between two possible interpretations of the nature of the distribution of correlation times. Equation 3 shows that the (nonexponential) autocorrelation function $\Phi(t)$ is just the Laplace transform of the distribution function $\rho(\tau)$. Yet, on the molecular level, two quite different mechanisms are possible. There may be a true distribution of correlation times: the rate of molecular processes may vary at different sites across the sample. But, in the limiting case, these rates do not change in time. That is, the density $\rho(\tau)$ implicitly describes some spatial inhomogeneity of individual Debye (single exponential) processes that, when averaged over the ensemble, lead to a nonexponential decay of the autocorrelation function. We shall refer to this type of distribution as an *inhomogeneous* distribution. The second possibility is that all the common molecular processes have an identical rate, but one which varies in time. In this case, each process is described by the same nonexponential autocorrelation function. Here the density $\rho(\tau)$ is just a mathematical convenience. This second type we call a *homogeneous* distribution. Certainly, both classes of distribution may coexist, and estimating which predominates is an experimental question.

Hence the identical autocorrelation function could arise by completely different routes of an inhomogeneous or homogeneous distribution. NMR line shape analysis can, in principle, distinguish between the two types of distributions.[22] Though the present results on the epoxy do not allow unambiguous discrimination, we shall conduct two parallel line shape analyses for inhomogeneous and homogeneous distributions.

(a) Inhomogeneous Distribution. For the inhomogeneous distribution, we adopt the view that there is a distribution of correlation times given by $\rho(\tau)$. A complete calculation would perform a weighted sum of the line shapes, eq 2, appropriate to a single relaxation time process for each value of τ. Instead we resort to a much simpler alternative. We approximate the line shape by an admixture of only two line shapes, those appropriate to the very fast and very slow processes.[20] Now, for the two-site exchange, there is some critical exchange time τ_x that defines the point of exact coalescence. This value is an NMR-defined boundary between fast and slow processes. Those processes with exchange times much less than τ_x will contribute a fully collapsed resonance line, while much slower processes contribute a line shape more appropriate to the rigid lattice. True, this segration does not properly account for those processes with correlation times near τ_x, but for a rather broad distribution, this error is not significant.[20] Further, the details of the actual shape of the distribution are not so important: the critical parameter is only the fast or slow fraction, defined in terms of τ_x. One merit of this approach is that a spectrum can be characterized by only one number, i.e., the fast fraction. When the spectral broadening is dipolar, then for a broad distribution of relaxation times a very broad line and a narrow (motionally narrowed) line can coexist. As temperature changes, the relative amplitudes of these lines change; Resing proposed and amplified the approach just outlined to explain this "apparent phase transition effect".[20,21]

The fast fraction F, the fraction of processes with correlation times shorter than τ, is calculated for the Williams–Watts function by integrating eq 6:

$$F(\tau/\tau_p) = \sum_1^\infty (-1)^{k-1} \frac{\Gamma(1 + k\alpha)}{k!} \left(\frac{\tau}{\tau_p}\right)^{k\alpha} \frac{\sin(\pi k\alpha)}{\pi k\alpha} \qquad (10)$$

The $\alpha = 0$ limit is again useful:

$$\lim_{\alpha \to 0} \{F(\tau/\tau_p)\} = 1 - \exp[-(\tau/\tau_p)^\alpha] \qquad (11)$$

Equivalently

$$\log [\ln (1 - F(\tau/\tau_p))^{-1}] = \alpha \log (\tau/\tau_p) \qquad (12)$$

In Figure 11 is a plot of log [ln $(1 - F)^{-1}$] against α log τ from eq 10; in the figure τ is measured in units of τ_p. The fast fraction F was calculated by computer from eq 10. For long relaxation times, convergence in the sum of eq 10 is quite slow and only a limited range of relaxation times is shown. However, even for large α, the limiting relation in eq 12 is nearly obeyed. For $\alpha = 0.3$, the deviation from linearity (dashed line) in Figure 11 is only about ±10% and hence the relations in eq 11 and 12 are nearly universal for $\alpha \leq 0.3$. One simple interpretation of τ_p is seen in Figure 11. Let τ_a be the correlation time for which log [ln $(1 - F(\tau_a))^{-1}] = 0$. At this point $F(\tau_a/\tau_p) = 1 - e^{-1}$: about 63% of the processes are faster than τ_a. We find by explicit calculation that $\tau_a \simeq 1.5\tau_p$ for all values of α.

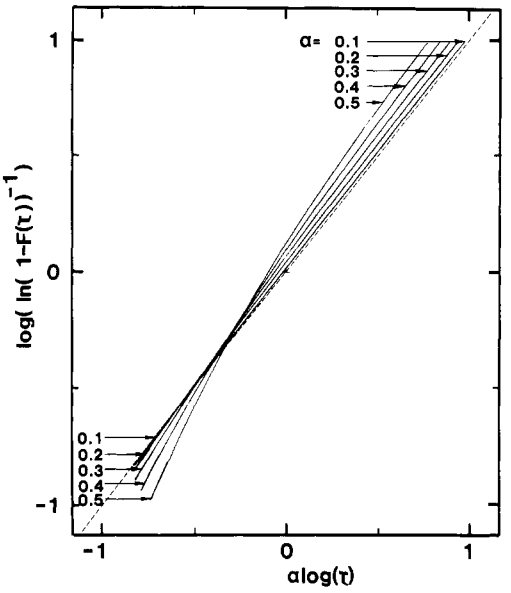

Figure 11. The fast fraction $F(\tau)$ represents the fraction of molecular processes with Debye correlation times shorter than τ. Here the fraction has been calculated from eq 10 for a Williams–Watts form of the autocorrelation function. In the figure, τ is measured in units of τ_p. The axes are chosen so that the $\alpha = 0$ limit is a straight line (dashed line in the figure).

The temperature dependence of the ^{13}C spectra of the piperidine-cured epoxy was analyzed for the inhomogeneous distribution as follows. Only peak d (of the carbons ortho to the oxygen) was considered since the scatter for peak c is too great. At each temperature the fast fraction was independently varied to produce a computer-simulated spectrum corresponding to that superposition of fast and slow components in best agreement with the observed spectrum. The spectra of the fast and slow components are given by the line shape of eq 2 in the limit of very fast or very slow exchange. The same peak separation and relaxation times were used as for the single relaxation time analysis (Table II). Single correlation time analysis had shown that the spectrum of carbon d coalesced for τ_x = 4.5 ms, corresponding to a temperature of 273 K. Hence the fraction derived from the data represents F(4.5 ms), the fraction of phenylene groups reorienting by 180° with correlation times faster than 4.5 ms. (Since this model is predicated on a broad distribution in relaxation times, the precise definition of τ_x is unimportant.)

For τ_p described by an Arrhenius relation, the $\alpha = 0$ limit of eq 12 becomes

$$\lim_{\alpha \to 0} \{\ln [\ln (1 - F(\tau/\tau_p))^{-1}]\} = \alpha[\ln (\tau/\tau_0) - E/RT] \quad (13)$$

Guided by this broad distribution limit, we plot ln (1 − $F(\tau_x)$)$^{-1}$ against reciprocal temperature on the semilogarithmic scale of Figure 12. The anticipated linear dependence is reasonably reproduced and the data are consistent within experimental error with the exp[$-(\tau/\tau_p)^\alpha$] form of the autocorrelation function.[39] In particular, the agreement is far more satisfactory than for the single relaxation time treatment of Figure 9: data above and below the coalescence point are reasonably fit. The slope in Figure 12 determines that $\alpha E = 18 \pm 2$ kJ/mol. The zero crossing ($F \simeq 0.63$) occurs at 295 K and, as previously indicated, corresponds to the point for which $\tau_a = \tau_x \simeq 1.5\tau_p$. Since τ_x = 4.5 ms, we have τ_p = 3 ms at 295 K. (The actual $\alpha = 0$ limit in eq 12 indicates that the zero crossing occurs at $\alpha \ln (\tau_a/\tau_p) = 0$ or $\tau_p = \tau_a$. We have chosen to use the $\alpha = 0$ limit to find αE but use the more exact expression, eq 10, to relate τ_p and τ_a. The slight differences

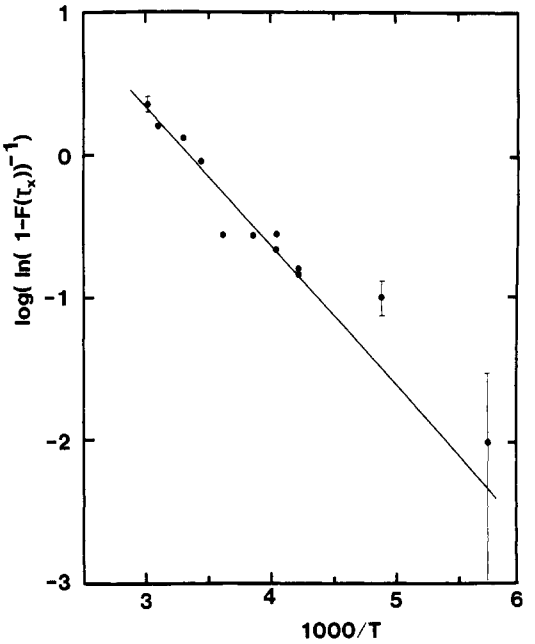

Figure 12. Temperature dependence of the fast fraction $F(\tau_x)$ describing the line shape of peak d in the piperidine-cured DGEBA epoxy; τ_x is the correlation time at coalescence (4.5 ms). An *inhomogeneous* distribution of relaxation times described by a Williams–Watts autocorrelation function is assumed.

in the numerical factors in τ_p are quite unimportant here.)

(b) Homogeneous Distribution. Here we presume that every phenylene group in the polymer is described by the nonexponential autocorrelation function $\Phi(t)$. The derivation of the line shape expression for two-site exchange is reported elsewhere.[22] The resulting line shape is

$$M(\omega) \propto \frac{AC + BD}{A^2 + B^2} \quad (14)$$

where

$$A = 1 - R_+R_- + S_+S_-$$

$$B = -(S_+R_- + S_-R_+)$$

$$C = (1 + R_-)U_+ + (1 + R_+)U_- - (S_+V_- + S_-V_+)$$

$$D = (1 + R_-)V_+ + (1 + R_+)V_- + (S_+U_- + U_+S_-)$$

$$R_\pm = \sum_i p_i(1 + \tau_i/T_{2\pm})/d_{i\pm}$$

$$S_\pm = \sum_i p_i(\omega \pm \delta\omega/2)\tau_i/d_{i\pm}$$

$$U_\pm = \sum_i p_i(1 + \tau_i/T_{2\pm})\tau_i/d_{i\pm}$$

$$V_\pm = \sum_i p_i(\omega \pm \delta\omega/2)\tau_i^2/d_{i\pm}$$

and $d_{i\pm} = [(\omega \pm \delta\omega/2)^2\tau_i^2 + (1 + \tau_i/T_{2\pm})^2]$. The plus/minus subscript refers to the two different sites. The p_i represent the weighting of the ith relaxation time. For the actual line shape calculation we used 33 values of τ_i, logarithmically spaced over 16 decades of relaxation times. The p_i are normalized by

$$p_i = G(\log \tau_i)[\log (\tau_{i+1}/\tau_i)] \quad (15)$$

so that

$$\sum_i p_i \simeq \int_{-\infty}^{\infty} d(\log \tau)\, G(\log \tau) = 1 \quad (16)$$

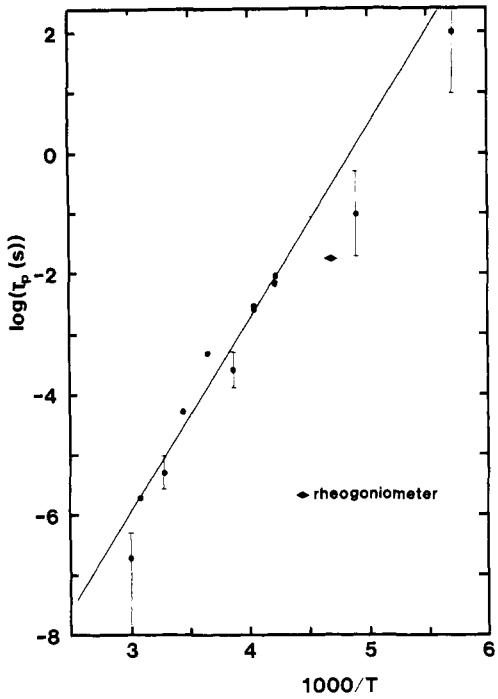

Figure 13. Temperature dependence of the correlation time τ_p for a description of the line shape changes in peak d of the piperidine-cured DGEBA spectrum in terms of a *homogeneous* distribution of correlation times described by a Williams–Watts autocorrelation function. In this figure a value of $\alpha = 0.28$ has been assumed.

As before, the correlation function is completely specified by the width parameter α and the correlation time $\tau_p = \tau_0 \exp(E/RT)$. Ideally, one might be able to determine α and τ_p independently at each temperature. The present suite of data does not allow this. Instead we assumed a temperature-independent value of α and then found the τ_p that, through eq 14, gave a best fit to each experimental line shape at each temperature. Figure 13 shows the results for $\alpha = 0.28$. The straight line in the figure represents an Arrhenius relation for τ_p with activation energy $E = 60$ kJ/mol (14 kcal/mol) and prefactor $\tau_0 = 4 \times 10^{-16}$ s. Other simulations with different α also gave reasonable Arrhenius relations for τ_p, out to values of α from 0.23 to 0.33 with corresponding activation energies E of 55–70 kJ/mol (13–17 kcal/mol).

v. Comparison of NMR Line Shape and Mechanical Relaxation Results. For the NMR data, only the temperature, not the frequency, could be changed. One consequence is that the distribution width parameter α cannot be determined independently, and the assumption of an Arrhenius relation for τ_p had to be made. For the NMR results, the assumption of a Williams–Watts-type autocorrelation function arising from an *inhomogeneous* distribution of correlation times gives the product $\alpha E = 18$ kJ/mol (4.3 kcal/mol). A homogeneous distribution of the same functional form gives $E = 60^{-5}_{+10}$ kJ/mol when α is assumed to be 0.28 ± 0.05, leading to $\alpha E = 17 \pm 1$ kJ/mol (4.1 ± 0.2 kcal/mol). The mechanical relaxation results yield $\alpha E = 18$ kJ/mol, with α and E independently determined as $\alpha = 0.28 \pm 0.02$ and $E = 63$ kJ/mol. The agreement among the mechanical results and the two treatments (inhomogeneous and homogeneous distributions) of the NMR results for the width parameter and temperature dependence of the distribution is within experimental error of about 10%. Hence, the phenylene reorientation and the mechanical loss processes are described by similar distributions, for at least they share a common product of αE.

The distribution of correlation times certainly fits the results far better than the single correlation time picture: note that the break point in the Arrhenius relation for the single correlation time model ($\alpha = 1$) of Figure 9 has essentially disappeared in Figures 12 and 13. Furthermore, the width of the mechanical relaxation β peak, Figure 10, can be interpreted only through a distribution of correlation times. However, the line shape analysis here is only reliable near coalescence. Much further away, the limited ^{13}C spectral resolution precludes accurate determination of the fast fraction F (Figure 12) or of the correlation time τ_p (Figure 13). As previously discussed, the resolution for peak d in this epoxy system is primarily determined by a distribution of isotropic chemical shifts and so is unlikely to be improved if higher magnetic field were available; perhaps in a deuterium rather than a ^{13}C study, one could distinguish between inhomogeneous and homogeneous distributions. For the inhomogeneous distribution, a collapsed line grows in at the center of the doublet as temperature is raised.[20-22] We may arbitrarily define coalescence as the point at which the amplitude of the central peak is just the average of the two outer peaks. If the resonance lines were very well-resolved and the T_2's of the two sites were identical, then the value of the fast fraction F would be $^1/_3$, indicating that one-third of the process have correlation times shorter than $\tau_{1/3}$, the correlation time at this coalescence point. Hence, for an inhomogeneous distribution an average correlation time similar to the *median* correlation time ($\tau_{1/2}$) determines coalescence. For the broad Williams–Watts distributions we find from Figure 11 that $\tau_{1/3} \ll \tau_p$; e.g., for $\alpha = 0.3$, $\tau_{1/3} = 0.04\tau_p$. Coalescence thus occurs for $\delta\omega\tau_p \gg 1$ for the inhomogeneous distribution.

On the other hand, for the homogeneous distribution, no central peak can be resolved.[22] Furthermore, the coalescence point is substantially shifted to longer times in the distribution. One may visualize the autocorrelation function of eq 4 as a description of a molecular process that starts out extremely rapidly at $t = 0$ and then slows down. In the context of the probability density $\rho(\tau)$, it looks as if the molecular process initiates at the very short τ region of the probability distribution and executes a glissando toward longer τ. Coalescence occurs only when the slowest effective process τ_s^{eff} satisfies $\tau_s^{eff}\delta\omega \simeq 1$, where the details of the relationship between τ_s^{eff} and τ_p depend on α, the peak separation $\delta\omega$, and the relaxation time T_2. In general, for $\alpha < 1$, $\tau_s^{eff} \gg \tau_p$ and hence, $\delta\omega\tau_p \ll 1$. Hence, coalescence is determined by the long-τ portion of the probability distribution. This observation applies to any homogeneous distribution, not just for the Williams–Watts distribution. This difference between correlation times derived from inhomogeneous and homogeneous distributions can be quite substantial and is illustrated in examining the correlation times found in this study.

Table III summarizes the distribution of correlation times inferred from the mechanical spectroscopy and the present NMR study. The actual correlation times are of particular interest. Both the Arrhenius prefactor and the interpolated or extrapolated room-temperature (295 K) correlation times are shown; the latter are less sensitive to errors in the determination of activation energy than is the Arrhenius prefactor.

Both the inhomogeneous and homogeneous distribution models provide reasonable fits to the data, Figures 12 and 13. Note that the correlation time τ_p at 295 K is 20 μs for the homogeneous distribution, rather than 3000 μs as for the inhomogeneous distribution: over 2 orders of magnitude separate the correlation times inferred from models

Table III
Williams-Watts Autocorrelation Function Parameters

	α	E, kJ/mol	αE, kJ/mol	τ_0, s	τ_p(295 K), μs
β transition[a] (mechanical relaxation)	0.28	63	18	7×10^{-18}	1
NMR line shape analysis (180° phenylene reorientation)					
inhomogeneous distribution	—	—	18[b]	2×10^{-14} [c]	3000
homogeneous distribution	0.28[d]	60	17	4×10^{-16}	20

[a] From analysis of the data of ref 31 and 32. [b] Determined only as the product. [c] Assumed mechanical relaxation activation energy of 63 kJ/mol to calculate τ_0. [d] Assumed. Reasonable fit for $\alpha = 0.28 \pm 0.05$.

with the same autocorrelation functions. This is a crucial point: the magnitude of correlation time inferred from NMR line shape studies depends critically on the homogeneous or inhomogeneous nature of the distribution of relaxation times. The mechanical loss spectrum, on the other hand, is independent of whether the distribution is homogeneous or inhomogeneous.

Table III shows the time scales for 180° phenylene reorientation and for mechanical relaxation to be rather different; at 295 K, values of τ_p are 1 μs (mechanical relaxation), 3000 μs (phenylene reorientation, inhomogeneous distribution), and 20 μs (phenylene reorientation, homogeneous distribution). We can *force* a reconciliation between the NMR and mechanical loss correlation times by the following arguments. Reorientation of the phenylene group by 180° was assumed to facilitate the line shape analysis: 180° rotation interchanges the protonated carbons across the ring, leading to a simple two-site exchange analysis. Certainly reorientation by steps less than 180° is possible, especially for a glassy polymer, and a more complete line shape analysis for jumps of less than 180° would require further knowledge of how the isotropic part of the carbon chemical shift varies with angle. Further, it is clear that pure 180° phenylene reorientations cannot account for mechanical relaxation since the ring is symmetrical about the 1,4 axis. If phenylene reorientation proceeded by small random steps (diffusive reorientation), then n^2 jumps of $(180°/n)$ would be required to reorient by the full 180°. If we associate the mechanical relaxation correlation time with these $(180°/n)$ jumps, then we can force agreement between the mechanical and NMR correlation times by letting $\tau_{NMR} = n^2\tau_{mech}$. Using the correlation times at 295 K, we find that the root-mean-square jump length is $180°/(3000/1)^{1/2} \simeq 3°$ for the inhomogeneous distribution and $180°/(20/1)^{1/2} \simeq 40°$ for the homogeneous distribution. This hypothesis provides one satisfactory reconciliation between the relaxation times determined by the mechanical data and the present NMR data. The phenylene reorientation through angles other than multiples of 180° can couple to the applied stress field to produce a mechanical relaxation. Certainly, the actual motions in this epoxy polymer may involve other motions superposed on the pure phenylene reorientation. But the present results show that phenylene reorientation takes place and that the distribution of relaxation times for the mechanical loss and NMR results are virtually coincident, provided we identify the mechanical process with 3° or 40° reorientation of the phenylene group, the choice depending on whether the distribution is inhomogeneous or homogeneous, respectively.

Summary and Conclusions

Cross-polarization and magic angle spinning methods were used to provide the ^{13}C spectra of four different phases of the DGEBA resin (liquid, crystalline, amorphous, and polymerized) and the temperature-dependent spectra of the polymer cured with piperidine, MPDA, HHPA, and NMA, respectively. Temperatures spanned 150–350 K for the polymers. In the crystalline resin, solid-state line splittings arise from the inequivalent sites. The high-field (3.5 T) spectrum showed clearly that more than one conformation or configuration of the monomer is present. The X-ray study[2] establishing the DGEBA crystal structure finds evidence that two conformations are available to the epoxide group at one end of the molecule; the other end does not have this freedom. The ^{13}C splittings expected for this structure were estimated by naive application of the steric hindrance model of Grant and Cheney[27] for hydrogen–hydrogen separations out to 0.25 nm; by this analysis the ^{13}C spectra present ambiguous evidence for the disordered epoxide ring, but there is no question that more than one form of the monomer is present. The estimated solid-state splittings do not agree in detail but are of the same magnitude as those observed (1–10 ppm).

In the piperidine-cured epoxy at low temperature, the resonances from the carbons ortho and meta to the oxygen each are seen as partly resolved doublets. At higher temperature these lines separately coalesce. This feature is seen in varying degrees in the other three epoxy polymers examined. It is shown that this coalescence is consistent with 180° reorientation of the phenylene ring. A single correlation time model shows that the effective correlation times are essentially equal, to within a factor of 2, for the meta and ortho carbons and therefore strengthens the argument that a common motion is responsible for the coalescence. The single correlation time model does not exhibit a simple Arrhenius temperature dependence; a break point occurs suspiciously near the coalescence point. This dilemma is resolved by appeal to a distribution of relaxation times, or equivalently, a nonexponentially decaying autocorrelation function to describe the molecular motion. The autocorrelation function chosen here is of the Williams–Watts form $\exp[-(t/\tau_p)^\alpha]$. It is shown that the probability distribution $\rho(\tau)$ and related mechanical susceptibility expression have a particularly simple form in the $\alpha = 0$ limit.

For NMR line shape analysis, we have considered two limits for the nature of the distribution describing the molecular motions in the polymer. An inhomogeneous distribution arises from a true (spatially varying) distribution of single-relaxation processes. In contrast, for a homogeneous distribution all common molecular processes are described by the same nonexponential autocorrelation function. Parallel application of these models to existing dynamic mechanical data and the present solid-state ^{13}C spectra for the piperidine-cured epoxy polymer shows that the shape (α) and temperature dependence (E) of the autocorrelation function are essentially identical for the mechanical relaxation process and 180° phenylene reorientation (Table III). The correlation times derived for 180° phenylene flips are longer than the mechanical relaxation time inferred from the same analysis. The NMR correlation times differ by a factor of 150 at 295 K, depending on whether a homogeneous or inhomogeneous

distribution is assumed; the present data do not distinguish between the two choices. The disparity in the NMR and mechanical relaxation results can be removed by assuming that the phenylene ring reorients by rotational diffusion with a root-mean-square jump of 3° (inhomogeneous distribution) or 40° (homogeneous distribution). Such jumps less than 180° do couple mechanically and may reflect one of the molecular processes responsible for the secondary relaxation in this epoxy polymer. Whether this is the actual loss mechanism and whether this process contributes in other bisphenol polymers will be better resolved as the highly specific information available from variable-temperature ^{13}C NMR supplements mechanical relaxation spectroscopy.

Acknowledgment. Thanks go to D. L. VanderHart and A. F. Yee for sharing their thoughts about motions in polymers. H. A. Resing encouraged us to appreciate the calculational and conceptual simplicity of the "apparent phase transition effect" model[20,21] for analyzing chemical exchange processes; G. C. Chingas and J. I. Kaplan helped to clarify features of distribution functions. C. F. Poranski, Jr., provided the liquid-state DGEBA spectrum. This work has been supported by the Naval Air Systems Command.

References and Notes

(1) Heijboer, J. "Mechanical Properties of Glassy Polymers Containing Saturated Rings", Communication No. 435, Central Laboratorium TNO: Delft, The Netherlands, 1972.
(2) Flippen-Anderson, J. L.; Gilardi, R. *Acta Crystallogr., Sect. B* **1981**, *B37*, 1433.
(3) Williams, G.; Watts, D. C. *Trans. Faraday Soc.* **1970**, *66*, 80.
(4) Ngai, K. L.; White, C. T. *Phys. Rev.* **1979**, *20*, 2475.
(5) (a) Ngai, K. L. *Comments Mod. Phys., Part B* **1979**, *9*, 127. (b) Ngai, K. L. *Ibid.* **1980**, *9*, 141.
(6) Lindsey, C. P.; Patterson, G. D. *J. Chem. Phys.* **1980**, *73*, 3348.
(7) Lowe, I. J. *Phys. Rev. Lett.* **1959**, *2*, 285.
(8) Hartmann, S. R.; Hahn, E. L. *Phys. Rev.* **1962**, *128*, 2042.
(9) (a) Beams, J. W. *Rev. Sci. Instrum.* **1930**, *1*, 667. (b) Andrew, E. R. *Arch. Sci. (Geneva)* **1959**, *12*, 103.
(10) Garroway, A. N.; Moniz, W. B.; Resing, H. A. *Org. Coat. Plast. Chem.* **1976**, *36*, 133.
(11) Garroway, A. N.; Moniz, W. B.; Resing, H. A. *ACS Symp. Ser.* **1979**, *No. 103*, 67.
(12) Sojka, S. A.; Moniz, W. B. *J. Appl. Polym. Sci.* **1976**, *20*, 1977.
(13) Poranski, C. F., Jr.; Moniz, W. B.; Birkle, D. L.; Kopfle, J. T.; Sojka, S. A. NRL Report No. 8092; Naval Research Laboratory: Washington, D.C., 1977.
(14) Garroway, A. N.; Moniz, W. B.; Resing, H. A. *Faraday Symp. Chem. Soc.* **1979**, *13*, 63.
(15) Garroway, A. N.; VanderHart, D. L.; Earl, W. L. *Philos. Trans. R. Soc. London, Ser. A* **1981**, *299*, 609.
(16) VanderHart, D. L.; Earl, W. L.; Garroway, A. N. *J. Magn. Reson.* **1981**, *44*, 361.
(17) Lyerla, J. R., personal communication (1979).
(18) Gutowsky, H. S.; Saika, A. *J. Chem. Phys.* **1953**, *21*, 1688.
(19) Gutowsky, H. S.; Holm, C. H. *J. Chem. Phys.* **1956**, *25*, 1228.
(20) Resing, H. A. *J. Chem. Phys.* **1965**, *43*, 669.
(21) Resing, H. A. *Adv. Mol. Relax. Processes* **1968**, *1*, 109.
(22) Kaplan, J. I.; Garroway, A. N. *J. Magn. Reson.*, in press.
(23) Schaefer, J.; Stejskal, E. O.; Buchdahl, R. *Macromolecules* **1977**, *10*, 384.
(24) Lippmaa, E. T.; Alla, M. A.; Pehk, T. J.; Engelhardt, G. *J. Am. Chem. Soc.* **1978**, *100*, 1929.
(25) Waugh, J. S.; Maricq, M. M.; Cantor, R. *J. Magn. Reson.* **1978**, *29*, 183.
(26) Steger, T. R.; Stejskal, E. O.; McKay, R. A.; Stults, B. R.; Schaefer, J. *Tetrahedron Lett.* **1979**, *4*, 295.
(27) Grant, D. M.; Cheney, B. V. *J. Am. Chem. Soc.* **1967**, *89*, 5315.
(28) Flippen-Anderson, J. L., personal communication (1980).
(29) Abragam, A. "Principles of Nuclear Magnetism"; Oxford University Press: London, 1961; pp 491ff.
(30) Kaplan, J. I.; Fraenkel, G. "NMR of Chemically Exchanging Systems"; Academic Press: New York, 1980; Chapter 6.
(31) Hunston, D. L.; Bascom, W. D.; Wells, E. E.; Fahey, J. D.; Bitner, J. L. In "Adhesion and Absorption of Polymers: Part A"; Lee, L.-H., Ed.; Plenum Press: New York, 1980; p 321.
(32) Hunston, D. L.; Carter, W. T.; Rushford, J. L. In "Developments in Adhesives"; Kinloch, A., Ed.; Applied Science Publishers: London, 1981; Chapter 4.
(33) Ting, R. Y., personal communication (1979).
(34) McCrum, N. G.; Read, B. E.; Williams, G. "Anelastic and Dielectric Effects in Polymeric Solids"; Wiley: London, 1967; Chapter 4.
(35) Nowick, A. S.; Berry, B. S. *Acta Met.* **1962**, *10*, 312.
(36) Williams, G.; Watts, D. C.; Dev, S. B.; North, A. M. *Trans. Faraday Soc.* **1971**, *67*, 1323.
(37) Reference 33, Chapter 4.
(38) Reference 6, Table I.
(39) These ^{13}C spectra are not sensitive to the details of the distribution: an alternative reasonable fit to these data is found for a log-normal distribution of correlation times. Resing, H. A.; Garroway, A. N.; Weber, D. C.; Ferraris, J.; Slotfeldt-Ellingsen, D. *Pure Appl. Chem.* **1982**, *54*, 595.

Magnetic Resonance and Relaxation in a Vinylidene Fluoride/Trifluoroethylene Copolymer

Vincent J. McBrierty,* Dean C. Douglass, and Takeo Furukawa†

Bell Laboratories, Murray Hill, New Jersey 07974. *Received December 2, 1981*

ABSTRACT: NMR T_1, T_2, and $T_{1\rho}$ relaxation data for poly(trifluoroethylene) (TrFE) and a 52/48 mol % vinylidene fluoride/trifluoroethylene copolymer (PVDF/TrFE) are reported. Three relaxations are observed in TrFE, in contrast to the two reported previously. The NMR results for the copolymer are broadly consistent with current interpretations of behavior in PVDF/TrFE reported in the literature. However, NMR reveals that both amorphous and crystalline regions are affected at the "70 °C transition". Immediately below the 70 °C transition the copolymer exhibits behavior that resembles that of glassy material.

Introduction

Considerable research effort has been expended in more clearly understanding the remarkable pyro- and piezoelectric properties of poly(vinylidene fluoride) (PVDF).[1,2] The trans-planar configuration of molecules, which characterizes the β polymorph (form I) is an important ingredient in achieving useful electrical properties. Not surprisingly, the copolymer of VDF with trifluoroethylene (TrFE)[3-5] is of special interest since TrFE in proportions greater than 10% induces the VDF component to preferentially crystallize in the β form.[5,6] Its properties are indeed intriguing and, in particular, a ferroelectric phase transition near 70 °C in the 55/45 mol % PVDF/TrFE copolymer has been proposed.[7] The transition is presumed to manifest cooperative rotation of dipoles in steps of $n\pi/3$ or $n\pi$.[1,2] The proposed ferroelectric transition is deduced

† Present address: The Institute of Physical and Chemical Research, 2-1 Hirosawa, Wako-Shi Saitama-Ken, 351, Japan.

0024-9297/82/2215-1063$01.25/0